ОРИГИНАЛЬНЫЕ ИССЛЕДОВАНИЯ

M. Nisa, S.A. Buzdar, F. Siddique, M.S. Ahmad, M. Akhtar, S. Nisar, A. Nazir, H. Ullah

DOI 10.25789/YMJ.2025.92.01

HARNESSING AI AND NATURAL THERAPEUTICS: COVID-19 DATA ASSESSMENT AND CURCUMIN'S ROLE IN MITIGATION

The main purpose of this work is to produce early finding /detection report for covid-19 by automated system using artificial intelligence techniques and drug development. This work comprises a proposed method for quantifying the features of textured Covid Images and Curcumin as an analyte for five various concentrations i.e. 0 mM, 10 mM, 20 mM, 30 mM and 40 mM. During data analysis using artificial intelligence and machine learning approaches, HRCT was found to be useful diagnostic tool. For the quantification and features extraction, statistical analytical methods were applied on normal and affected data (grey images) after discussion with expert radiologist. Total number of region of interests selected was 320. The proposed method accuracy for three classes COVID-19 mild cases, COVID-19 severe cases and normal cases were 94.4%, 96.6% and 98.4%. Sensitivity was 94.5%, 96.6% and 98.4% with respect to principal component analysis, linear discriminant analysis and nonlinear discriminant analysis. Clinical findings disclose the higher mortality rate, different severity levels and to identify the stages of virus attack. Curcumin can be used as drug to improve histopathological results.

Keywords: Covid-19, Texture analysis, Curcumin, Co-occurrence matrix

For citation: Nisa M., Buzdar S.A., Siddique F., Ahmad M.S., Akhtar M., Nisar S., Nazir A., Ullah H. Harnessing AI and Natural Therapeutics: COVID-19 Data Assessment and Curcumin's Role in Mitigation. Yakut medical journal. 2025; 92(4): 5-13. https://doi.org/10.25789/YMJ.2025.92.01

Introduction: There was a huge viral attack, checked in December 2019, appeared in Wuhan, province Hubei China and firstly spread to the other regions of china and then to the worldwide [1]. This novel corona virus (COVID-19) was observed with some common symptoms in mild cases like fever, fatigue, dry cough, etc. and in serious cases, infections observed that can cause fatal pneumonia [2], dyspnea, and acute respiratory distress condition that lead to death [3]. According to literature survey COVID-19 can spread among humans by means of respiratory track [4-5]. It was observed that mortality ratio was low in children [6] and high in males and elderly persons [7]. The incubation period for COVID-19 varies based on different sources: WHO (The World Health Organization) reported duration for incubation period for corona virus 2-10 days while, NHC (China's National Health Commission) had announced the estimated incubation duration 10-14days. The CDC (United States) claimed 2-14days whereas DXY.cn, a top ranked Chinese online community for physicians and health care professionals, reported estimation 3-7 days can be up to 14 days. The effective way to reduce the strength of corona virus is proper isolation [1]. Today's basic necessity is to identify the early stage of COVID-19 (even before symptoms appear) with an automated report generation with collaboration of diagnostic imaging. Literature shows Texture analysis plays great role in segregating the pattern observed in medical images [8-9]. CT texture analysis is a prominent tool to investigate and identify human tissue features precisely to distinguish malignant and normal tissue images by applying different quantification methods [10].

COVID-19 is a disease that spreads through virus and triggers the Severe Acute Respiratory Syndrome (SARS). In December 2019 COVID-19 spreads in whole world with origin Wuhan, a city of China [11]. Many elucidations were conducted on genome of COVID-19 by scientists and made many drugs. Protease was selected for such drugs because it works when RNA of Covid-19 replicates [12]. Curcumin is one of the most prominent antiviral. Bisdemethoxycurcumin, desmethoxycurcumin and curcuminoid are three types of curcumin. It is a polyphenol [13]. Curcumin acts as anticancer, antidepressant, antioxidant, anti-inflammatory and antiviral in many biological phenomenon's [14]. Curcumin by the process of fibrosis during COVID-19 reverse the pathway of pulmonary system due to its biological targets like inflammatory response, inhibition and immunological properties [15]. We have discussed the biological components and parameters of blood of COVID-19 patient for 0 mm, 10 mm, 20 mm, 30 mm and 40 mm hematological under Curcumin analyte.

The infected CT images of COVID-19 showed similarity for chest tomographic configuration of ground glass opacities, consolidation with bilateral and marginal lung infections for SARS-CoV-19. The radiologist found similar symptoms in detecting abnormalities for viral pneumonia and SARS-CoV-19 Pneumonia [16].

There is limitation in chest CT findings due to its negative prognostic value at primary symptoms appearance [17]. Artificial intelligence (AI) is somehow performing better understanding in human imaging analysis as well as for identifying abnormalities [18]. According to literature survey Coronavirus belongs to one of the largest viruses group Nidovirales, which contains Coronaviridae, Arteriviridae, Mesoniviridae, and Roniviridae families [19]. The Coronavirinae comprise of nine families. These viruses firstly differentiate or grouped according to serology

NISA Mehrun – PhD, Assistant Professor, Department of Physics, Govt. Sadiq College Women University, Bahawalpur, Pakistan; **BUZDAR Saeed Ahmad** – PhD, Professor, Institute of Physics, The Islamia University of Bahawalpur, Bahawalpur, Pakistan, **SIDDIQUE Farzana** – M. Phil, Assistant Professor, Department of Physics, Lahore Garrison University, Sector C, DHA Phase 6, Lahore, Pakistan; **AHMAD Muhammad Saeed** – PhD, Assistant Professor, Department of Physics, Govt. Sadiq College Women University, Bahawalpur, Pakistan; **AKHTAR Munir** – PhD student, Institute of Physics, The Islamia University of Bahawalpur, Bahawalpur, Pakistan; **NISAR Sarah** – MBBS, Medical Doctor, Department of Diagnostic Radiology, Bahawal Victoria Hospital, Bahawalpur, Pakistan; **NAZIR Aalia** – PhD, Associate Professor, Institute of Physics, The Islamia University of Bahawalpur, Bahawalpur, Pakistan; **ULLAH Hafeez** – PhD, Associate Professor, Institute of Physics, The Islamia University of Bahawalpur, Bahawalpur, Pakistan

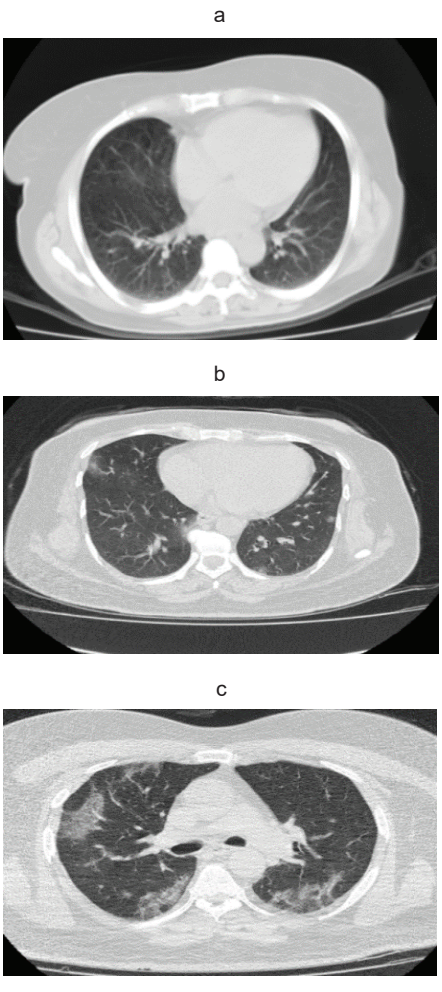

Fig. 1. High Resolution Computed tomography (HRCT) images of (a) normal and COVID-19 infected data (b) mild cases and (c) severe cases

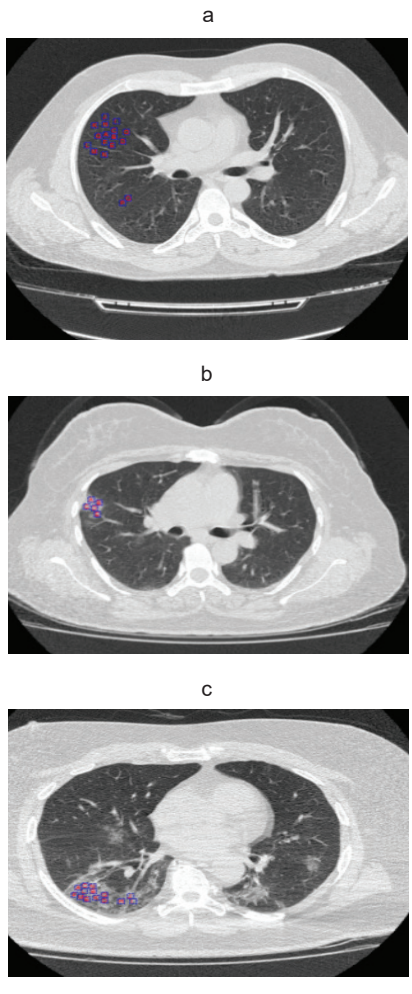

Fig. 2. ROI marked on HRCT images of the patients (a) normal (b) mild infected with covid (C) severe with coronavirus disease-2019. In case(c) GGO, consolidation and septal thickening appear that reveals the severity

but now they are classified by phylogenetic assembling. The Coronaviruses Alpha, Beta, Gamma and Delta are the four species arises from Coronavirinae family [20]. Lu et al [21] studied that a novel coronavirus (termed 2019-nCoV) detected during clinical sample investigations from viral pneumonia patients in Wuhan, China. 2019-nCoV has resemblance in pattern with the virus caused by SARS, epidemic 2003. A novel research on COVID-19 is also given by one of the academy of Medical Sciences in China described by Ren et al. They observed this research in five patients that was diagnosed with pneumonia due to viral as the major reason, later tested COVID-19 positive with the metagenomics observation of samples of patients of respiratory tract. Sequence findings showed that this virus is phylogenetically closest to the bat SARS-like CoV, but is in a different lineage, possessing. In addition, the amino acid sequence of this new CoV's preliminary receptor-binding domain (RBD) resembles that of SARS-CoV, implying that the same receptor could be used.

According to Wang et al [22], for the development to study and get rid of this dangerous and complex virus, scientific study is of critical importance. Many development and advance research, in field of medical, environmental and science, is needed to understand the clear view, growth and transfer of virus in body.

Rao *et al.* suggested that if online mobile based app is discovered to take sample, patient history, critical symptoms of COVID-19, it will save time and fast isolation is possible [23]. Even this data can be used for the basic screening and rapid detection of COVID-19 patients. With the help of artificial intelligence (AI), a statistical calculation can be achieved that will give good information according to risk factors like patients having no risks, patients having low risk, patients having medium risk factor and patients with severe risk. The patients with severe -risk factor detected may then be quarantined sooner, minimizing the probability of the virus spreading. It is very necessary to communicate with children and families in the hospitals. People may feel that there is no COVID-19 treatment, but we need to help them realize that it

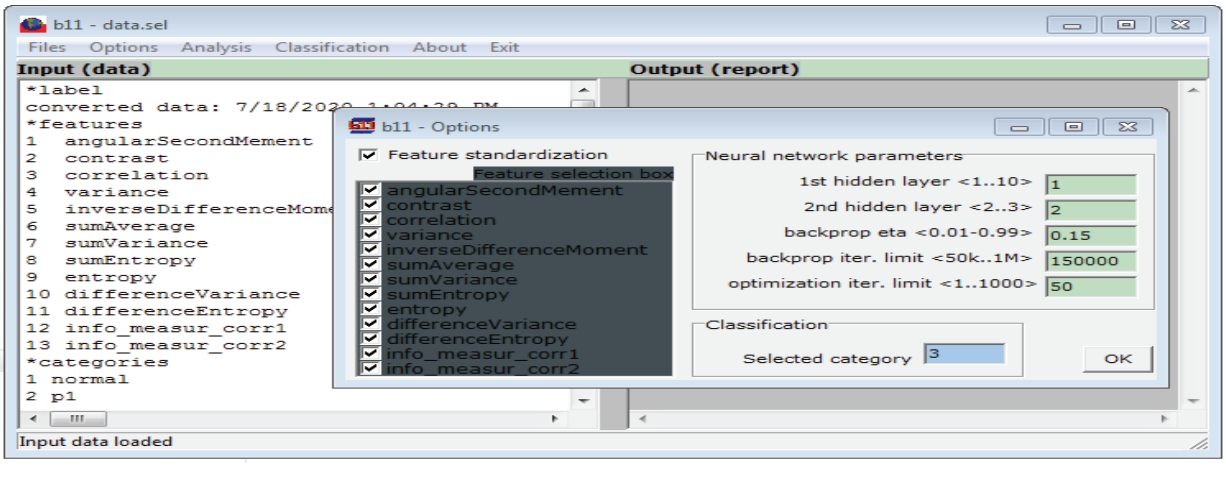

Fig. 3. Showing feature selection box using B11 software.

is likely that positive therapy is all that is required [6].

To estimate the transmission risk of COVID-19, a mathematical model was proposed to conclude that 6.47 could be the basic reproduction number. Wang et al. [24] proposed the following guidelines, based on the report findings (1) CT scan or x-ray scan of lung of each patient should be considered. In clinically suspected cases of quarantine, patients with traditional pulmonary signs should be included. Lung CT should be rechecked in 3 to 5 days for patients without apparent lung signs but with clinical symptoms, (2) as a requirement for admission to the quarantine ward, positive lung CT results instead of a positive nucleic acid test should be used. (3) CT exams should be performed every 5 to 7 days in hospitalized patients and a low-dose scan should be used. In short, clinicians and radiologists should recognize the importance of chest CT in the diagnosis and treatment of COVID-19, be familiar with the characteristics and diagnostic points of COVID-19 chest imaging, and improve contact within the radiology community, which is particularly important in the fight against COVID-19 [24].

Currently researchers are working on AI (Artificial Intelligence) to develop tools that can boost the potential of health care [18]. *Qanees et al.* developed FPASSA-ANFIS (flower pollination algorithm using the salp swarm algorithm) that was applied as a forecasting technique that has the ability to predict number of confirmed COVID-19 cases within ten days [25]. Srinivasa *et al.* suggested that deep learning algorithms can be implemented to identify early signs of COVID-19 viral infection [23].

Materials and methods. In this study, the data was collected from personal contacts for clinical aspects to characterize and differentiate normal and COVID-19 cases. Analysis was done with 20 normal cases versus 20 corona infected patients with mild state and 50 severe corona patients with HRCT images. Senior doctors and radiologist were consulted for the precise judgment and discussion of symptoms and clinical findings to strengthen proposed analysis results. The most common symptoms observed in mild cases were fever, cough, fatigue, myalgia (body aching) and poor appetite. Clinical findings were peripheral Ground Glass Opacity (GGO), Basal Consolidation, septal thickening and vascular dilation [26] etc. Recovery time was 10-15 days. Severe patients were observed with some complications due to diabetics, hypertensive, cardiac, smoker, high grade fever and shortness of breath. Some patients were treated with oxygen therapy. Pattern on HRCT was same Ground glass opacity, consolidation, septal thickening and vascular dilation with high grade. Recovery time examined 21 days to one month. Generally, age was one of the basic factors perceived in mortality rates.

Blood smear preparation: Blood smear method was used for preparation of slides of blood cells. Fixing and staining was used for WBCs and RBCs and for platelet cells PRP by centrifuge method at 50×10^6 rpm. Fixing is done by using Ethanol and staining by using field strain (A, B). Then images of these slides were captured by using microscope with lens of 40X for WBCs and RBCs. This was conducted at room temperature.

Feature Extraction: The digitization of texture features is done by feature extraction process in texture analysis methods. Texture variation, angles of direction and surface structure can be defined by these extracted features or parameters. Statistical analysis method, Co-occurrence matrix was used for computing Haralick texture features for each ROI. Features data was calculated from the region of interests was based on image intensity. A square matrix that keeps record of frequencies of occurrence of these gray levels in pairs relationships is known as co-occurrence matrix [27]. Its dimensions are independent to that of the image matrix [28].

Grey level co-occurrence matrix is second order method that statistically measures grey level. It works with the linear spatial relationship between neighboring pixels and describes combinations with neighboring pixels exist in any direction at angle θ [10, 29-30]. The computed Haralick texture features are *Angular Second Moment*, Contrast, Correlation, Variance, Inverse Difference Moment, Sum Average, Sum, variance, Sum Entropy, Entropy, Difference Variance, Difference Entropy, Information Measures of Correlation I, and Information Measures of Correlation2.

Experimental Results. High Resolution Computed tomography (HRCT) was performed with patients using 64-slice Toshiba Medical System, X-ray high voltage generator, Model CXXG-012A, input was 3˜, 200V and 50/60 Hz. Maximum input power was 90kVA. The output was 120kV, 600mA, and 135kV, 530mA made in Japan.

Selection and construction of ROIs. Region of interests were defined or selected when image loaded on image processing software. In this research work system was defined region of interest with sizes 8 × 8, 16 × 16 and 32 × 32 window sizes. For the precision and accuracy 8 × 8 ROI was constructed. Multiple ROIs from patient's image were chosen to increase the number of number of samples from patient's data. Size of region of interest basically indicates the number of pixels under consideration. In this study the shape of the selected region of interest was square.

Feature Selection. In digital image total dimensions are proportional to the number of pixels exist in that pattern. In that sense it constructs large number of dimensions. For specific problems it is good to minimize the number of dimensions by making feature vector. That features are called the statistical parameters which describes the spatial interrelationship of different grey levels in neighboring pixels. Basically feature section or reduction makes sense in terms of grouping

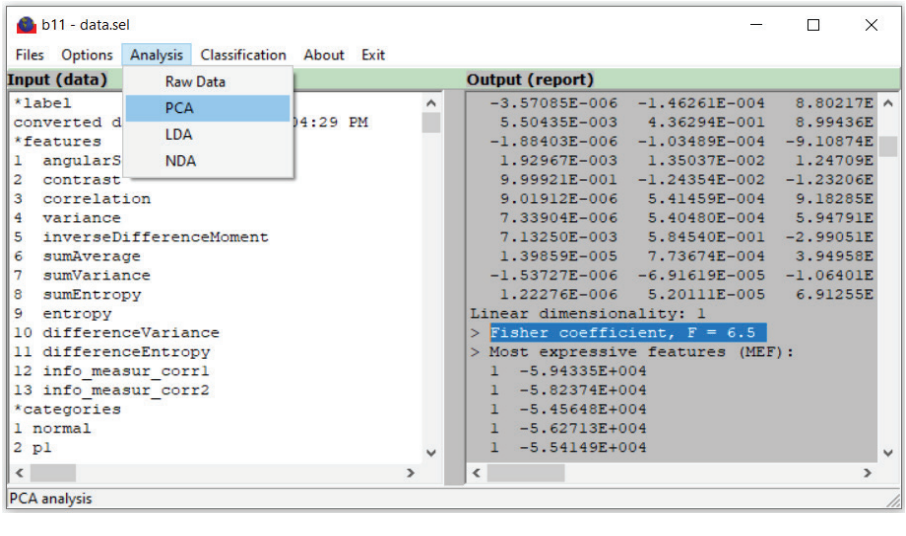

Fig. 4. showing analysis techniques using B11 software

Таблица 1

Features	pooled mean	pooled standard deviation
angular Second Moment	5.8036E-03	5.5229E-03
contrast	7.6720E+02	5.2918E+02
correlation	3.4903E-01	2.3780E-01
variance	5.3339E+02	3.6326E+02
inverse Difference Moment	1.0860E-01	1.2192E-01
sum Average	2.6590E+02	7.9759E+01
sum Variance	7.6099E+04	4.0695E+04
sum Entropy	4.2502E+00	5.8819E-01
entropy	5.5698E+00	5.8719E-01
difference Variance	6.2831E+02	4.4838E+02
difference Entropy	3.4639E+00	8.1990E-01
info_measur_corr1	-3.6850E-01	8.8901E-02
info_measur_corr2	9.3751E-01	7.8914E-02
Statistical Techniques	**Results**	
Principle component Analysis		
Linear dimensionality	5	
Fisher coefficient	11.6	
Feature vector standardization	yes	
1-NN classification of MEFs:		
Misclassified data vectors	18/320 [or 5.63%]	
Linear Discriminant analysis		
Linear separability	0.98	
LDA dimensionality	2	
Fisher coefficient	181	
Feature vector standardization	yes	
1-NN classification of MDFs:		
Misclassified data vectors	11/320 [or 3.44%]	
Nonlinear discriminant analysis		
Misclassified f. vectors	5/320 [or 1.56%]	
Fisher coefficient, F	50.4	
Feature vector standardized	yes	

or sorting to reduce irrelevant data and approach to accuracy. This feature selection process applied before the statistical techniques are applied on data [31].

Statistical Assessment / Data Processing Techniques. Statistical analysis was executed using Sante DICOM viewer (used to view images on impartial system), IrfanView 64 (that is pronounced for viewing and accomplishing trivial image's management. It simply works from changing file format to manipulation of digital images basic features), computer vision lab [32] (software designed for PhD work, used to compute different region of interest with 8 by 8, 16 by16, and 32 by 32 cursor size) and B11 [29] (a unit/software permits visualization of sample distribution and sorting the feature vectors. Furthermore, it provides tool for artificial neural network (ANN) and nonlinear supervised classification (1NN-1-nearest neighbor classifier). Statistical techniques executed in the B11 software encompass PCA (Principal component analysis), LDA (Linear discriminant analysis) and NDA (nonlinear discriminant analysis) [33-35].

Texture Analysis. Texture analysis is considered as the excellent tool in medical field like radiology. Homogenous and heterogeneous textures are pronounced in medical images for pointing the same and violent nature of lesions in the diagnostic imaging. To study diagnostic images, there is vital need to understand image pathology in detail. An image is

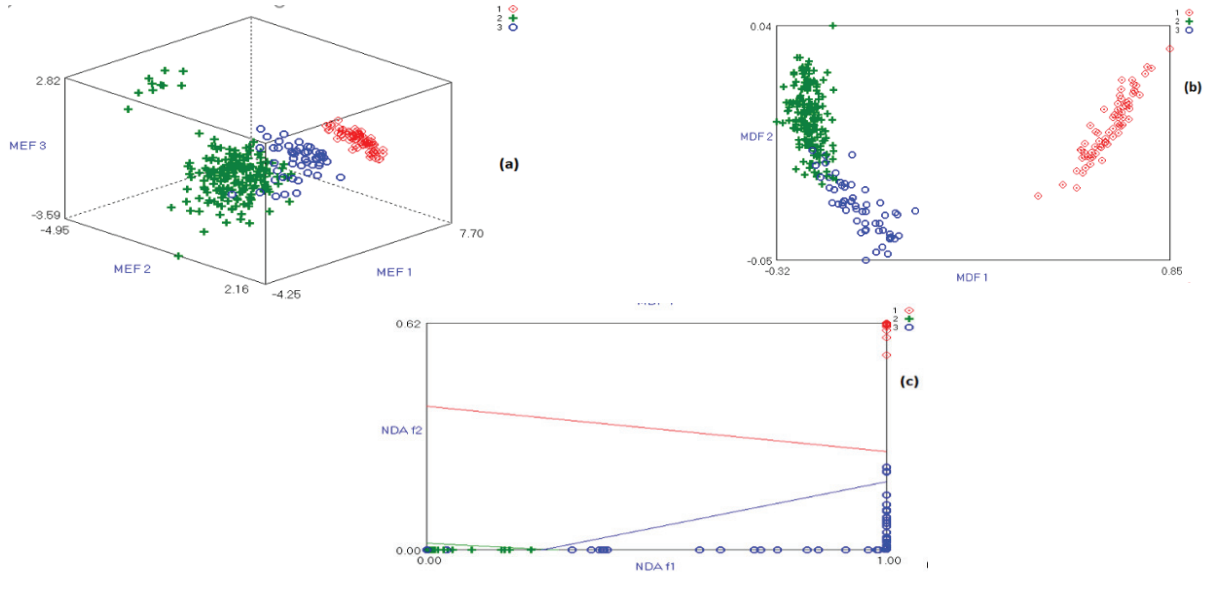

Fig. 5. Showing the distribution of texture features for ROI of dimensions 8 * 8 within normal (marked as red) and Covid (with severe cases marked as green) and with mild states (marked as blue) by (a) Principle Component Analysis in three dimensions, The longitudinal, lateral and vertical axis corresponds to most expressive features (MEFI, MEF2 and MEF3) (b) Linear Discriminant Analysis in two dimensions, The horizontal and vertical axis corresponds to the most Discriminative features in one linear dimension(MDF1 and MDF2) (c) Nonlinear Discriminant Analysis in two dimensions (NDAf1 and NDAf2).

collection of unit cell called pixel [36]. In latest research texture analysis has become the fundamental part of radiology to measure different parameters. As the images can be homogenous or heterogeneous (shows complicated pattern for crucial stages), for the quantification of heterogeneity, texture analysis is the essential tool that defines the texture information, that can predict routine stages and survival rates against diseases [32, 37]. The proposed method for this work figures out results from Haralick texture features using statistical techniques deduced from Co-occurrence matrix (GLCM). As single pixel intensity value variation does not provide enough information about texture behavior that's why second order statistics is used for pair of pixels.

Results showing Haralick texture features with pooled mean (p. mean) and pooled Standard deviation (p.std) and for all these features different statistical techniques Principle component analysis, Linear Discriminant analysis and Non-linear discriminant analysis presenting normalization, fisher Coefficients and misclassification rates (normal versus COVID-19 textured data) with feature vector standardization and 1NN classification of MEFs (Table 1).

(a) showing confusion matrix for classification using Principle component analysis (PCA) (b)Differentiation performance of normal versus covid (mild and severe cases) table showing the overall accuracy 94.4% with application of texture analysis method.TP, TN, FP and FN represent true positive, true negative, false positive and false negative respectively (Table 2).

(a) showing confusion matrix for classification using Linear discriminant analysis (LDA) (b) differentiation performance of normal versus covid (mild and severe cases) table showing the overall accuracy 96.6% with application of texture analysis method. TP, TN, FP and FN represent true positive, true negative, false positive and false negative respectively. (Table 3).

(a) showing confusion matrix for classification using Non discriminant analysis (NDA) (b) differentiation performance of normal versus covid (mild and severe cases) table showing the overall accuracy 98.4% with application of texture analysis method. TP, TN, FP and FN represent true positive, true negative, false positive and false negative respectively. (Table 4).

Microscopic Results. Deviations of blood components and parameters under five different concentrations of Curcumin i.e. 0 mM, 10 mM, 20 mM, 30 mM and 40 mM by using white light microscope of sample set (II) are shown below in figure 6.

Discussion. Figure 1 represents the overall workflow adopted in this research, illustrating the sequential steps involved in image acquisition, preprocessing, feature extraction, and classification. Initially, HRCT (High-Resolution Computed Tomography) or polarimetric images of patients were acquired and stored in a digital format. These images were then subjected to preprocessing operations, including noise reduction, contrast enhancement, and normalization, to ensure uniformity across all sam-

Таблица 2

a

PCA Analysis
TRUE Class

Predicted Class	Normal	Severe	Mild
Normal	71	0	0
Severe	0	186	10
Mild	0	8	45

b

PCA							
Class Name	TP	TN	FP	FN	Precision	Recall	F1-Score
Normal	71	249	0	0	1.000	1.000	1.000
Severe	186	116	10	8	0.949	0.959	0.954
Mild	45	257	8	10	0.849	0.818	0.833
Total	302		18	18	0.944	0.944	0.944

Таблица 3

a

LDA Analysis
TRUE Class

	Normal	Severe	Mild
Normal	71	0	0
Severe	0	190	7
Mild	0	4	48

b

LDA							
Class Name	TP	TN	FP	FN	Precision	Recall	F1-Score
Normal	71	249	0	0	1.000	1.000	1.000
Severe	190	119	7	4	0.964	0.979	0.972
Mild	48	261	4	7	0.923	0.873	0.897
Total	309		11	11	0.966	0.966	0.966

Таблица 4

a

NDA Analysis
TRUE Class

Predicted Class	Normal	Severe	Mild
Normal	71	0	0
Severe	0	194	5
Mild	0	0	50

b

NDA							
Class Name	TP	TN	FP	FN	Precision	Recall	F1-Score
Normal	71	249	0	0	1.000	1.000	1.000
Severe	194	121	5	0	0.975	1.000	0.987
Mild	50	265	0	5	1.000	0.909	0.952
Total	315		5	5	0.984	0.984	0.984

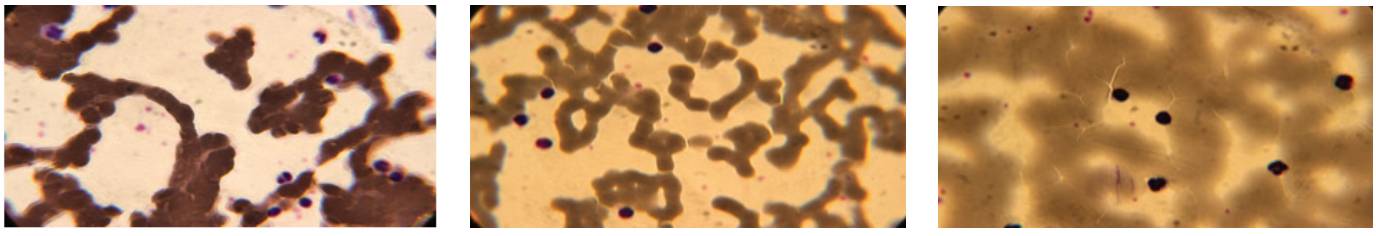

Fig. 6. Micrograph showing size and shape changes of WBCs fewer than five concentrations of Curcumin i.e. 0mM to 40mM under analyte (curcumin) at 40X.

Таблица 5

Abnormalities or improvement in cells and parameters values under Curcumin Concentrations

Sr. No.	Curcumin Concentration mM	No. of WBCs 10^3 /µL	No. of platelet 10^3 /µL	No. of RBCs 10^6/ µL	HGB g/dL	RDW %	PDW %	MCV fL	MPV fL	HCT %	PCT %
1	0 mM	2.85	178	4.05	10.2	15.4	18.9	92.4	8.2	37.3	0.24
2	10 mM	4.17	219.5	4.33	10.6	15.9	20.6	93.5	8.6	37.1	0.24
3	20 mM	4.99	245.7	4.41	10.5	15.7	20.1	94.1	8.0	39.2	0.20
4	30 mM	7.69	246	4.58	12.1	15.8	21.9	94.9	8.6	42.3	0.23
5	40 mM	10.47	280.9	4.89	14.3	16.4	22.3	96.6	8.5	44.6	0.25

ples. Subsequently, texture-based and statistical parameters were extracted from the processed images to quantify microstructural differences between normal and infected tissues. The extracted features were then analyzed using dimensionality reduction and classification techniques such as PCA, LDA, and NDA to distinguish between various stages of infection or disease severity. Thus, Figure 1 outlines the complete analytical pipeline—from raw image input to final diagnostic classification—demonstrating the systematic approach adopted in this study. Figure 2 depicts the selection of **Regions of Interest (ROIs)** on HRCT images of patients with varying degrees of COVID-19 infection. Subfigure **(a)** represents a normal lung image showing clear alveolar structures without visible abnormalities. Subfigure **(b)** shows a mildly infected case, where faint **ground-glass opacities (GGO)** are observed, indicating early inflammatory changes. Subfigure **(c)** illustrates a severely infected lung, where extensive **GGO**, **consolidation**, and **interlobular septal thickening** are evident, signifying advanced pulmonary involvement and severe tissue damage. The ROIs were marked as square windows of fixed size to capture specific texture patterns within each region, facilitating quantitative comparison of structural changes across infection stages. This figure demonstrates the rationale behind ROI selection and highlights the visual progression of COVID-19–related pathological features in HRCT imaging.

In the present study, total number of regions of interest selected for work was 320, in which normal were 71, mild 55 and severe 194. The pooled statistical evaluation of polarimetric texture features demonstrated clear distinctions between normal and pathological tissues. High contrast (7.67×10^2) and variance (5.33×10^2) indicated significant structural heterogeneity, while low angular second moment (5.80×10^{-3}) and inverse difference moment (0.108) reflected reduced uniformity. Elevated entropy (5.57) and sum entropy (4.25) values signified increased randomness and tissue disorganization associated with malignancy. Correlation parameters (0.349) and information measures (info_measure_corr1 = –0.368; info_measure_corr2 = 0.938) confirmed moderate pixel dependencies, highlighting disrupted microstructural patterns. Principal Component Analysis (PCA) achieved a Fisher coefficient of 11.6 with 5.63% misclassification, while Linear Discriminant Analysis (LDA) improved accuracy (3.44% error; Fisher = 181; separability = 0.98). The best classification was obtained using Nonlinear Discriminant Analysis (NDA), showing only 1.56% misclassification and Fisher coefficient of 50.4. Overall, nonlinear statistical mapping demonstrated superior tissue differentiation and strong diagnostic potential of polarimetric and textural parameters. Here the proposed work has done with ROI 8*8. As indicated in table 1, p. mean and p.std was derived from Haralick texture features. After setting feature vectors standardization, neural network parameters, and classifying categories, analysis was completed with PCA, LDA and NDA methods. In PCA model the linear dimensionality and fisher coefficient were 5 and 11.6 respectively.1-NN classification of MEFs shows the misclassification data vectors 5.63% and classification and overall accuracy for PCA module was 94.4% (as indicated in table 2) Figure 3(a) showing the distribution of texture features for ROIs for normal cases the isolated cluster is observed (red) with 100 % accuracy while other two clusters showed accuracy with some misclassification proportion. These disparities measured by means of other physical aspect ratio (symptoms of unhealthy conditions like smoking, hypertension and diabetes etc.). Figure 3(b) showing the distribution of texture features for normal, mild and severe ROIs there is three sequestered clusters, but Covid-infected was lineup in comparison with normal that showed the aggressive nature of disease even in mild or critical situation. In LDA model the linear separability was 0.98. LDA dimensionality was 2 and fisher coefficient was 181. During 1-NN classification of MDFs the misclassification rate was observed 3.44%. The overall accuracy perceived was 96.6%for LDA analysis (as shown in table 3). In NDA analysis fisher coefficient was 50.4 and misclassified f. vectors were 1.56%. The overall accuracy 98.4% was reported (as point out in table 4). Even though there was overlapping among some ROIs among mild and severe cases that showed the variation of infection rates due to already existed some dysfunctions of the body. While the analysis with normal cases was reported 100% for all methods PCA, LDA

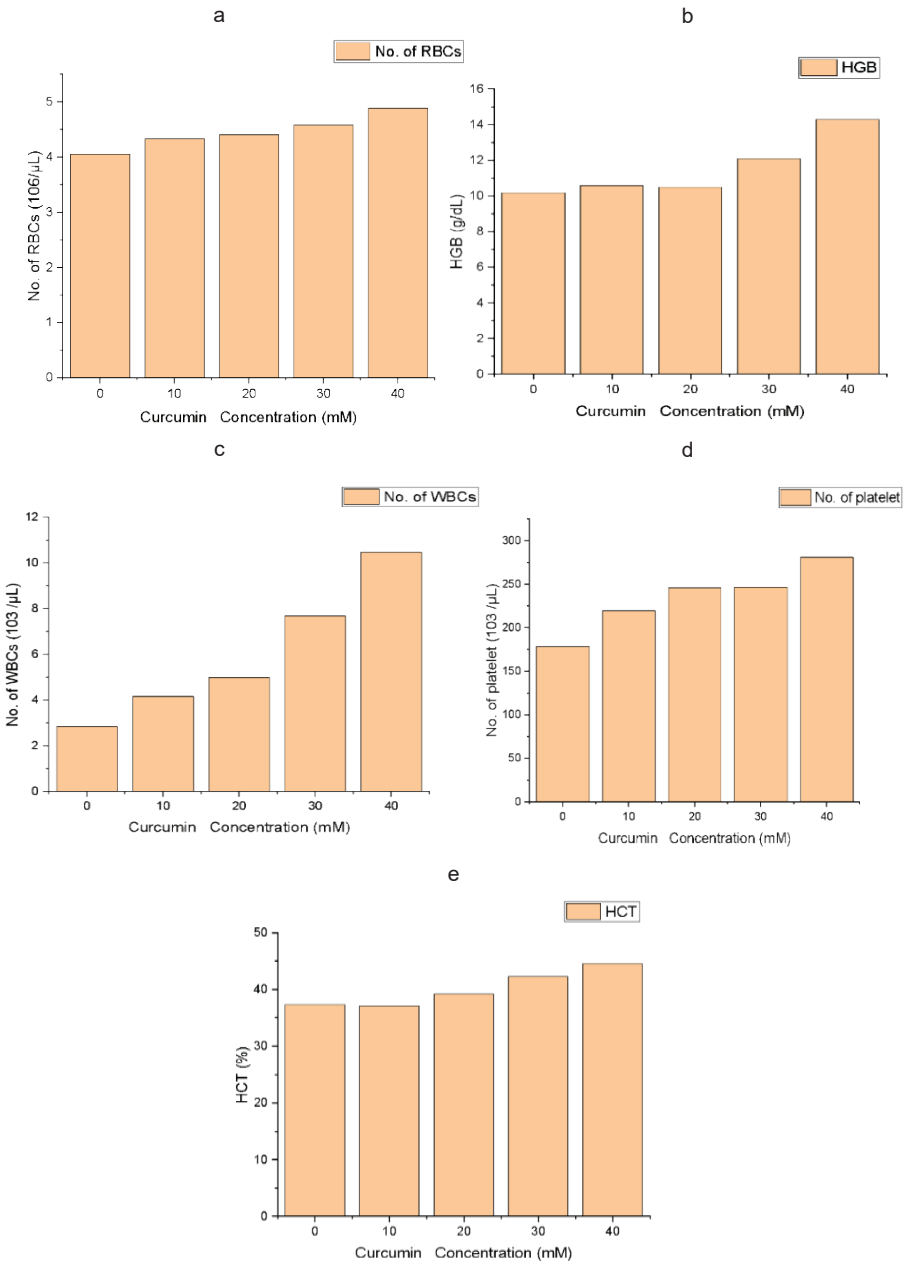

Fig. 7. Showing two dimensional graphical trends of (a) WBC (b) PLTs (C) RBCs (d) HGB and (e) HCT against 0 mM to 40 mM concentration of Curcumin Analyte with step size of 10 mM.

and NDA. Figure 3(c) discriminated the texture features properly due to contrast and correlation of the vectors.

In this proposed work different confusion matrices have drawn for the real assessment. These matrices are showing TP, TN, FP and FN (true positive, true negative, false positive and false negative) values with measurements of Precision, Recall, F1-score and accuracy (used equations are shown below [38].

Precision = TP/(TP+FP) (1)
Recall/ Sensitivity = TP/(TP+FN) (2)
*F1-score = (2*TP)/(2*TP+FP+FN)* (3)
Overall accuracy = Sum of TP/ Total number of ROI (4)

Accuracy (https://tech.labs.oliverwyman.com/blog/2019/10/17/accuracy-precision-recal-elixir/) is the sum of the diagonal divided by the total. Table 2(a) is showing the confusion matrix for PCA analysis, the TP (True positive) for normal was 71, TN (True negative) 249, FP (False positive) and FN (False negative) was 0. Value of Precision, recall and F1-score was 1 that shows excellent accuracy for normal ROIs for PCA. For severe cases/ samples/ ROIs the TP was 186 and TN 116 whereas FP and FN values were 10 and 8 respectively. Precision, recall and F1 score was less than 1 and 0.949, 0.959 and 0.954 respectively. For mild ROIs TP was 45 and TN, FP and FN was 257, 8 and 10 respectively. Measurements for precision with recall and F1 score was less than 1 and 0.849, 0.818 and 0.833 respectively. Table 2 (b) presenting the total TP= 302, FP and FN =18, total precision = recall = F1-score = 0.944. The overall accuracy calculated from the confusion matrix was 94.4%.

Table 3 presenting a confusion matrix for LDA analysis to differentiate between performance of normal versus covid (mild and critical) ROIs. Value of TP=71, TN = 249, FP=FN=0 and precision, recall and F-1 score approaches to 1, that shows the maximum accuracy. In case of severe category TP=190, TN= 119, FP=7, FN=4 and the values of the precision, recall and f1-score were 0.964, 0.979 and 0.972 respectively. For mild class TP=48, TN=261, FP=4, FN=7, precision= 0.923, recall=0.873, and F1-score was 0.897. LDA analysis showed more vibrant results as compared to PCA with total TP 309, FP=FN=11, overall precision was 0.966, recall 0.873 and F1-score 0.966 that disclosed the total accuracy 96.6%.

Confusion matrix for NDA method has drawn in Table 4 that delivers the descriptive information about textural features of different ROIs. In normal case like PCA and LDA precision was observed with excellent results with 100% TP and TN ratio. In severe class TP was 194, TN 121, FP and FN was reported with values 5 and 0 respectively. In this analysis value of precision was 0.975, Recall 0.909 and F1-score 0.952. In mild category the values for TP, TN, FP and FN were 50, 265, 0 and 5 respectively. Precision points to 1 whereas recall and F1-score were 0.909 and 0.952 respectively. NDA analysis presented more exciting results with entire accuracy of 98.4% and total precision was 0.984. Although the total TP values were 315 and FP, FN were 5, 5 respectively. It is concluded that Corona virus is an extremely spreadable among human beings and can cause moderate to prolonged effects that can be harmful [39]. Patients with mild state observed with ground glass opacity (GGO) and basal consolidation in common. GGO was the most common sign in either mild or severe patients. In critical situations lesions were scattered and finally infected the lungs and septal thickening and vascular dilation were found with pulmonary consolidation. These changes appear in the form of shortness of breath that takes time to recovery and enhance infection rate. This suggests that presented techniques have promising probability to identify the infection in early stages even on critical one. The visual assessment/ findings indicate that mortality rate can

be increased due to aging, or lesions present in lungs or liver [2-3, 40] or others. It is also cleared at this stage that HCRT texture analysis is a practically applicable tool for characterization and differentiation normal versus infected ROIs. In further recommendations that are a lot of work remaining on individual diseased organs infected with covid-19 that will help out to more commercialize this method in diagnostic units.

Also we have tried to explain the abnormalities / improvement in blood cells and parameters of Covid-19 patient blood with the help of hematology and microscopy after admixing Curcumin for inherent concentration i.e. 0 mM and for 10 mM, 20 mM, 30 Mm and 40 mM. Convicted covid-19 patient has highly effected immune system and blood coagulation system i.e. physiology of WBCs and Platelet cells are disturbed highly. Size and shape of WBCs is improved by the use of curcumin as we can see from figure 5 (a-e). Shape of RBCs changes from biconcave to spherical and spiked and their size also increases when we increase the concentration of Curcumin. Similarly, size and shape of Platelet cells is improved under curcumin from inherent to optimum value as shown in figure 6 (a-e). Count of WBCs goes on increasing gradually from 8.5**×**10^3/μL at inherent value to 8.94**×** 10^3/μL at optimum value as drawn in figure 7 (a). Basophil and lymphocytes illustrate drastic changes. Thus Curcumin improves the immune system of Covid-19 patient. Lymphocytes (natural germ killer) produce antibodies against the parts affected by either cancer or by virus. Their count increases from 2.23% to 4.74%. Basophil produces histamine (homeostasis factor) and heparin (an anticoagulant). Count of Basophil cells is also increased from 0.55% to 2.57% as we mix curcumin from inherent to optimum concentration. Rest types of WBCs remained unchanged. In covid-19 patient count of platelet cells goes on increasing from 178×10^3/μL at inherent value and reaches 280.9×10^3/μL at 40 mM concentration as drawn in figure 7(b). It can also be concluded that low count of platelet cells in diabetes can be improved by using curcumin. Count of RBCs in Covid-19 patients is not much affected just very slow gradual increase. HGB is the oxygen transportation pigment of Red colour present in our body. HGB level increases as we increase the concentration from 10.2 g/dL at inherent value up to14.4 g/dL at optimum value as drawn in figure 7(d). Respiratory system suffered a lot in covid-19 but Curcumin plays very vital role in restoring it by increasing the HGB level. Parameter like HCT which measures the proportion of RBCs in blood is increased from 37.3% to 44.6% as we increase the concentration of Curcumin. Parameters like MCV, MPV, RDW, PCT and PDW show little bit deviation at optimum value as we compare with value at inherent concentration. Thus, Curcumin showed a strong restorative effect on the hematological profile of COVID-19 patients. Increasing its concentration improved the morphology and count of WBCs, RBCs, and platelets**,** enhancing immune response, oxygen transport, and blood coagulation balance. Elevated HGB and HCT levels, along with increased lymphocyte and basophil counts, confirm curcumin's role in strengthening immunity and restoring normal blood physiology. Overall, curcumin demonstrates promising potential as a natural therapeutic agent for mitigating hematological disturbances caused by COVID-19 infection.

Conclusion. This study has total 320 ROIs, with normal 71; mild 55 and severe 194 by using after setting feature vectors standardization, neural network parameters, and classifying categories, analysis was completed with PCA, LDA and NDA methods. The results show an excellent accuracy for normal ROIs for **PCA** with TP=71, TN=249, FP and FN was 0 and precision value=1. Severe cases for PCA with TP=186, TN=116, FP=10and FN=8 and precision value <1 while Mild cases for PCA with TP=45, TN=257, FP=8and FN=10 and precision value <1. The overall accuracy calculated from the confusion matrix was **94.4%**. For **LDA** analysis of normal ROIs TP=71, TN = 249, FP=FN=0 and precision approaches to 1,. In case of severe category TP=190, TN= 119, FP=7, FN=4 and the values of the precision <1. For mild class TP=48, TN=261, FP=4, FN=7, precision <1. LDA analysis showed more vibrant results as compared to PCA that disclosed the total accuracy **96.6%**. For **NDA** in normal case like PCA and LDA precision was observed with excellent results with 100% TP and TN ratio. NDA analysis presented more exciting results with entire accuracy of **98.4%**. It is concluded that Corona virus is an extremely spreadable among human beings and can cause moderate to prolonged effects that can be harmful and Curcumin has the potential as one of the most prominent, less expensive, homeopathic antiviral for improvement of blood cells and parameters in Covid-19 patient.

Declarations. Formal consent was not required, as the study used archived, anonymized diagnostic samples and CT data without patient contact or intervention, in accordance with institutional ethical guidelines.

Competing interests: The authors declare that they have no competing interests

Data Availability: Raw data and derived data supporting the findings of this study are available from the corresponding author on request.

Funding: This research did not receive any specific grant from funding agencies in the public, commercial, or not-for-profit sectors.

Литература

1. Abdullah Farid, A., G.I. Selim, and H.A.A. Khater, A Novel Approach of CT Images Feature Analysis and Prediction to Screen for Corona Virus Disease (COVID-19), in Preprints. 2020, Preprints.

2. Boeckmans, J., et al., COVID-19 and drug-induced liver injury: a problem of plenty or a petty point? Archives of toxicology, 2020; 94(4): 1367-1369.

3. Parohan, M., S. Yaghoubi, and A. Seraji, Liver injury is associated with severe coronavirus disease 2019 (COVID-19) infection: A systematic review and meta-analysis of retrospective studies. Hepatology Research, 2020; 50(8): 924-935.

4. Liu, K.-C., et al., CT manifestations of coronavirus disease-2019: A retrospective analysis of 73 cases by disease severity. European Journal of Radiology, 2020. 126.

5. Lu, C.-w., X.-f. Liu, and Z.-f. Jia, 2019-nCoV transmission through the ocular surface must not be ignored. The Lancet, 2020. 395(10224): p. e39.

6. Zachariah, P., COVID-19 in Children. Infectious Disease Clinics of North America, 2022; 36(1): 1-14.

7. Liu, R., et al., Positive rate of RT-PCR detection of SARS-CoV-2 infection in 4880 cases from one hospital in Wuhan, China, from Jan to Feb 2020. Clinica Chimica Acta, 2020; 505: 172-175.

8. Scalco, E. and G. Rizzo, Texture analysis of medical images for radiotherapy applications. British Journal of Radiology. 2017; 90(1070).

9. Goyal, A. and R. Gunjan, Bleeding Detection in Gastrointestinal Images using Texture Classification and Local Binary Pattern Technique: A Review. E3S Web Conf., 2020; 170: 03007.

10. Dhruv, B., N. Mittal, and M. Modi, Study of Haralick's and GLCM texture analysis on 3D medical images. International Journal of Neuroscience, 2019; 129(4): 350-362.

11. Wang, C., et al., A novel coronavirus outbreak of global health concern. The Lancet, 2020; 395(10223): 470-473.

12. Zhang, X.W. and Y.L. Yap, Old drugs as lead compounds for a new disease? Binding analysis of SARS coronavirus main proteinase with HIV, psychotic and parasite drugs. Bioorganic & medicinal chemistry, 2004; 12(10): 2517-2521.

13. Dourado, D., et al., Will curcumin nanosystems be the next promising antiviral alternatives in COVID-19 treatment trials? Biomedicine & Pharmacotherapy, 2021; 139: 111578.

14. Minassi, A., et al., Dissecting the Pharmacophore of Curcumin. Which Structural Element Is Critical for Which Action? Journal of Natural Products, 2013; 76(6): 1105-1112.

15. Zahedipour, F., et al., Potential effects of curcumin in the treatment of COVID-19 infection. Phytotherapy Research, 2020; 34(11): 2911-2920.
16. Borges do Nascimento, I.J., et al., Novel Coronavirus Infection (COVID-19) in Humans: A Scoping Review and Meta-Analysis. Journal of Clinical Medicine, 2020; 9(4): 941.
17. Bernheim, A., et al., Chest CT Findings in Coronavirus Disease-19 (COVID-19): Relationship to Duration of Infection. Radiology, 2020; 295(3): 685-691.
18. Davenport, T. and R. Kalakota, The potential for artificial intelligence in healthcare. Future Healthcare Journal, 2019; 6(2): 94-98.
19. Shchelkanov, M.Y., et al., History of investigation and current classification of coronaviruses (Nidovirales: Coronaviridae). Russian journal of Infection and Immunity, 2020; 10(2): 221-246.
20. Fehr, A.R. and S. Perlman, Coronaviruses: An Overview of Their Replication and Pathogenesis, in Coronaviruses: Methods and Protocols, H.J. Maier, E. Bickerton, and P. Britton, Editors. 2015, Springer New York: New York, NY.1-23.
21. Lu, R., et al., Genomic characterisation and epidemiology of 2019 novel coronavirus: implications for virus origins and receptor binding. The Lancet, 2020; 395(10224): 565-574.
22. Wang, J.-W., B. Cao, and C. Wang, Science in the fight against the novel coronavirus disease 2019 (COVID-19). Chinese Medical Journal, 2020; 133(9): 1009-1011.
23. Srinivasa Rao, A.S.R. and J.A. Vazquez, Identification of COVID-19 can be quicker through artificial intelligence framework using a mobile phone–based survey when cities and towns are under quarantine. Infection Control & Hospital Epidemiology, 2020; 41(7): 826-830.
24. Wang, K., et al., Imaging manifestations and diagnostic value of chest CT of coronavirus disease 2019 (COVID-19) in the Xiaogan area. Clinical Radiology, 2020; 75(5): 341-347.
25. Al-qaness, M.A.A., et al., Optimization Method for Forecasting Confirmed Cases of COVID-19 in China. Journal of Clinical Medicine, 2020; 9(3): 674.
26. Ng, M.-Y., et al., Imaging Profile of the COVID-19 Infection: Radiologic Findings and Literature Review. Radiology: Cardiothoracic Imaging, 2020; 2(1): e200034.
27. Low, A., Introductory Computer Vision and Image Processing. 1991: McGraw-Hill.
28. Eleyan, A. and H. Demirel. Co-occurrence based statistical approach for face recognition. in 2009 24th International Symposium on Computer and Information Sciences. 2009.
29. Strzelecki, M., et al., A software tool for automatic classification and segmentation of 2D/3D medical images. Nuclear Instruments and Methods in Physics Research Section A: Accelerators, Spectrometers, Detectors and Associated Equipment, 2013; 702: 137-140.
30. Qadri, S., et al., A Comparative Study of Land Cover Classification by Using Multispectral and Texture Data. BioMed Research International, 2016; 2016(1): 8797438.

The full version of the list of references is in the editorial office.

DOI 10.25789/YMJ.2025.92.02

УДК 618.36-06
(576.31+576.344):616.155.12]Covid-19

И.А. Андриевская, Т.С. Чурикова, О.Л. Кутепова

ГИСТОЛОГИЧЕСКИЕ ИЗМЕНЕНИЯ ПЛАЦЕНТЫ ПРИ ХРОНИЧЕСКОЙ СУБКОМПЕНСИРОВАННОЙ ПЛАЦЕНТАРНОЙ НЕДОСТАТОЧНОСТИ У ЖЕНЩИН С COVID-19 СРЕДНЕЙ СТЕПЕНИ ТЯЖЕСТИ ВО ВТОРОМ И В ТРЕТЬЕМ ТРИМЕСТРАХ БЕРЕМЕННОСТИ

Проведено гистологическое изучение тканей плаценты у женщин с хронической субкомпенсированной плацентарной недостаточностью, ассоциированной с COVID-19 средней степени тяжести. Исследование позволило выявить следующие нехарактерные специфические признаки вирусного повреждения тканей: децидуальная васкулопатия, лимфоплазмоцитарная инфильтрация, тромбы в венозных сосудах стволовых ворсин, виллит и интервиллузит, отложение межворсинчатого фибриноида, гиперплазия синцитиотрофобласта и хорангиоз. Морфометрический анализ показал повышение доли периворсинкового фибрина и капилляров в терминальных ворсинах, снижение плотности синцитиокапиллярных мембран. Дополнительно установлено увеличение количества синцитиальных узелков и промежуточных незрелых ворсин, а также полнокровие капилляров в промежуточных и терминальных ворсинах. Среднетяжелое течение COVID-19 во втором и в третьем триместрах беременности ассоциируется со структурными изменениями в плаценте, которые при недостаточной эффективности компенсаторно-приспособительных механизмов являются одной из причин развития хронической субкомпенсированной плацентарной недостаточности

Ключевые слова: беременность, COVID- 19, хроническая субкомпенсированная плацентарная недостаточность, гистология плаценты, морфометрия

The histologic study of placental tissues in women with subcompensated chronic placental insufficiency associated with moderate COVID-19 was conducted. Histologic study of placenta from women of the main group revealed the following uncharacteristic specific signs of viral tissue damage: decidual vasculopathy, lymphoplasmacytic infiltration, thrombi in the venous vessels of the stem villi, villitis and intervillusitis, deposition of intervillous fibrinoid, hyperplasia of syncytiotrophoblast and chorangiosis. Morphometric analysis showed an increase in the proportion of perivorsinchal fibrin and capillaries in terminal villi, and a decrease in the density of syncytiotrophoblast membranes. In addition, an increase in the number of syncytial nodules and intermediate immature villi, as well as capillary bleeding in intermediate and terminal villi were found. The moderately severe course of COVID-19 in the second and third trimesters of pregnancy is associated with structural changes in the placenta, which, with insufficient efficiency of compensatory and adaptive mechanisms, is one of the causes of the development of subcompensated chronic placental insufficiency.

Keywords: pregnancy, COVID- 19, chronic placental insufficiency, placental histology, morphometry

Для цитирования: Андриевская И.А., Чурикова Т.С., Кутепова О.Л. Гистологические изменения плаценты при хронической субкомпенсированной плацентарной недостаточно-

ФГБНУ «Дальневосточный научный центр физиологии и патологии дыхания» (675000, г. Благовещенск, ул. Калинина, 22): **АНДРИЕВСКАЯ Ирина Анатольевна** – д.б.н., зав. лаб., irina-andrievskaja@rambler.ru, ORCID 0000-0003-0212-0201, **ЧУРИКОВА Татьяна Сергеевна** – м.н.с., churikova97@yandex.ru, ORCID 0009-0002-9893-2799, **КУТЕПОВА Ольга Леонидовна** – к.б.н., н.с., helga1509_84@mail.ru, ORCID 0000-0002-8895-3943.